Advance Sustainable Science, Engineering and Technology (ASSET)
Vol. 8, No.4, October 2026, pp. 02604023-01 ~ 02604023-011
ISSN: 2715-4211 DOI: https://doi.org/10.26877/asset.v8i4.2712

Structural and Electronic Characterization of Hexose Crystals: Insights into Crystal Packing and Hydrogen-Bonding Based on Crystal Density and Molecular Orbital Analysis

Tomoko Takashita[1*], Ryunosuke Takata[1], Mizuki Aoe[1], Kei Takeshita[2], Tomohiko Ishii[1]

[1]Graduate School of Science for Creative Emergence, Kagawa University, 2217-20 Hayashi-cho, Takamatsu, Kagawa 761-0396, Japan.

[2]Fushimi Pharmaceutical Co Ltd, 307 Minatomachi, Marugame, Kagawa 763-8605, Japan.

*s25d154@kagawa-u.ac.jp

Abstract. Rare sugars are monosaccharides and their derivatives that occur only in trace amounts in nature, with diverse applications anticipated in food, medicine, and agriculture. In recent years, their structural diversity has attracted increasing attention for potential applications in materials science. Although all hexoses share the same chemical formula ($C_6H_{12}O_6$), differences in OH group orientation can significantly alter density, crystal packing, and hydrogen bonding patterns. In this study, thirteen hexoses were analyzed to evaluate the relationship between OH group orientation and crystal density, and to quantitatively assess hydrogen bond strength using Bond Overlap Populations (BOP) calculated via the DV-Xα method. The crystal densities ranged from 1.55 to 1.68 g cm^{-3}, and the BOP values typically fell within the 10^{-2}-electron range, indicating moderate hydrogen bond interactions. These findings quantitatively demonstrate how subtle stereochemical variations govern crystal structures and intermolecular interactions, providing fundamental insights for designing sugar based functional materials.

Keywords: Bond Overlap Population, crystal density, crystal packing, DV-Xα molecular orbital calculation, rare sugars

(Received 2025-09-10, Revised 2026-07-30, Accepted 2026-08-01, Available Online by 2026-10-31)

© 2026 The Author(s). Advance Sustainable Science, Environmental Engineering and Technology (ASSET) are published under the terms of the Creative Commons Attribution-ShareAlike (CC BY-SA 4.0). Authors retain the copyright to their work. Users may read, copy and distribute the work in any medium provided the authors and the journal are appropriately credited

1. Introduction

Monosaccharides are broadly classified into “natural sugars,” which are abundant in nature, and “rare sugars,” which occur only in trace amounts. The International Society of Rare Sugars defines rare sugars as “monosaccharides and their derivatives that exist only in limited quantities in nature” [1]. In recent years, rare sugars have attracted considerable attention due to their unique biological activities, which are absent in natural sugars, making them promising candidates for applications across medicine, food, and agriculture [2-6]. For example, the representative rare sugar D-psicose has been reported to exert blood glucose–lowering effects [7], while D-allose exhibits antitumor activity and immunomodulatory properties [8-10]. Moreover, D-tagatose, in addition to its use in food products, has been reported to function as an “edible pesticide” capable of suppressing plant diseases [11], further expanding the scope of rare sugar applications. Beyond these bioactivities, recent attention has increasingly focused on their structural characteristics, offering potential for the development of functional materials.

Hexoses such as glucose and fructose share the same molecular formula ($C_6H_{12}O_6$) yet adopt diverse three-dimensional structures due to differences in the stereochemical orientation of their OH groups. Such subtle structural variations have a pronounced impact on crystal structures, particularly in terms of intermolecular hydrogen bonding and molecular packing, making them critical factors in the utilization of monosaccharides as functional materials.

In crystalline materials, physical properties are strongly influenced by molecular packing arrangements and electronic interactions such as hydrogen bonding. Therefore, elucidating the effects of subtle differences in the OH group orientation on intermolecular interactions is essential for understanding the structural and interactional characteristics of monosaccharides and for guiding their rational design as functional materials.

Recent crystallographic and computational studies have shown that differences in functional groups or their spatial arrangement can lead to changes in hydrogen bond networks and packing arrangements in molecular crystals, including sugar derivatives and bioactive ligands [12, 13]. These examples illustrate that subtle structural variations significantly influence supramolecular organization. However, most such analyses rely primarily on geometric descriptions, and electronic perspectives on intermolecular interactions remain limited. In particular, systematic, quantitative comparisons of hydrogen bond strength across hexoses are still scarce, which motivates the need for complementary approaches capable of evaluating both geometric and electronic features.

To address this gap, this study integrates crystallographic analysis with electronic structure calculations. Thirteen hexoses, including both natural and rare sugars, were examined to evaluate the relationship between OH group orientation and crystal density. Furthermore, intermolecular hydrogen bond strengths were quantitatively assessed using Bond Overlap Populations (BOP) derived from DV-Xα molecular orbital calculations. By combining geometric and electronic perspectives, this work aims to elucidate how subtle stereochemical differences influence crystal packing and intermolecular interactions, thereby advancing the understanding of structure–interaction relationships in monosaccharide crystals.

2. Methods

In this study, the crystal structures and intermolecular interactions of thirteen hexoses were systematically investigated [14-26]. The crystal structures used in this work were obtained from the Cambridge Structural Database (CSD), and the corresponding CSD reference codes for all thirteen hexoses are as follows: β-D-allose (CCDC 1129030), β-D-altrose (CCDC 722033), β-D-glucose (CCDC 1169302), β-D-mannose (CCDC 1450809), β-D-gulose (CCDC 903430), β-D-galactose (CCDC 1107362), α-D-glucose (CCDC 1500503), α-D-talose (CCDC 1101363), α-D-galactose (CCDC 1101282), β-D-fructose (CCDC 1902789), β-D-psicose (CCDC 776516), α-L-sorbose (CCDC 1262281), and α-D-tagatose (CCDC 738284). Because these datasets originate from experimentally

determined single-crystal X-ray structures, hydrogen atom positions were used exactly as deposited in each CSD entry without additional refinement.

To evaluate crystal packing characteristics, crystallographic data of six β-aldohexoses were retrieved from the CSD, including the molecular structures, crystal densities, lattice parameters, and molecular orientations. These data were analyzed to examine how variations in hydroxyl group orientation influence crystal density.

To quantitatively assess intermolecular interactions—particularly hydrogen bond strengths—molecular orbital calculations were carried out for all thirteen hexoses using the DV-Xα method [27-29]. As a first-principles molecular orbital framework, the DV-Xα method does not involve software versioning. The model system consisted of a central molecule surrounded by 8–10 neighboring molecules arranged in a cluster configuration so as to preserve the hydrogen bond network observed in the crystal. Self-consistent field (SCF) calculations were repeated until the change in orbital populations fell below 0.00001 *e*, ensuring sufficient convergence of the electronic structure.

The hydrogen bond strengths were expressed as BOP, which numerically represent the degree of overlap between the wavefunctions of two atoms; higher values indicate stronger hydrogen bonding. For typical hydrogen bonds, the BOP values are on the order of 10^{-2} electrons. In accordance with international conventions, the six oxygen atoms in each hexose ring are numbered from O1 to O6, as illustrated in Figure 1, and these designations are used consistently throughout this paper.

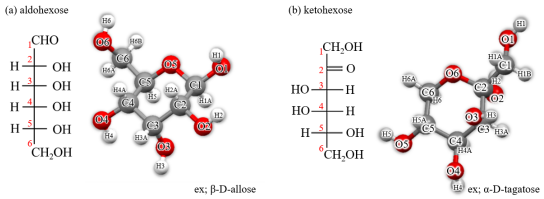


Figure 1. Numbering scheme for the oxygen atoms in hexoses.
(a) aldohexose (example: β-D-allose).
(b) ketohexose (example: α-D-tagatose).

3. Results and Discussion

This study discusses the crystal densities and molecular orbital calculations of thirteen hexoses. The target crystal structures, obtained from the Cambridge Structural Database (CSD) as detailed in Section 2, serve as the basis for the analysis. The molecular structures are shown in Figure 2, and the unit cell parameters are listed in Tables 1 to 3.

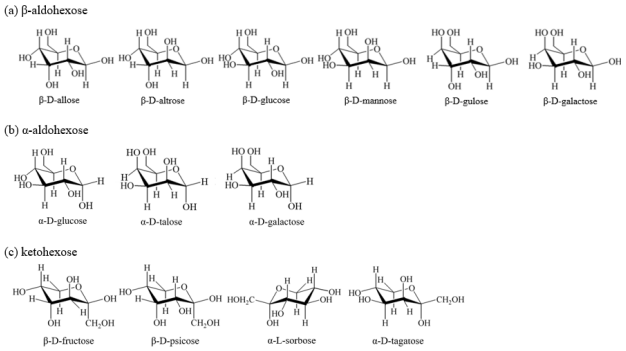


Figure 2. Molecular structures of the 13 hexoses examined in this study.
(a) β-aldohexoses (6 species).
(b) α-aldohexoses (3 species).
(c) ketohexoses (4 species).

Table 1. Unit cell parameters of β-aldohexoses.

	β-D-allose	β-D-altrose	β-D-glucose	β-D-mannose	β-D-gulose	β-D-galactose
Formula	$C_6H_{12}O_6$	$C_6H_{12}O_6$	$C_6H_{12}O_6$	$C_6H_{12}O_6$	$C_6H_{12}O_6$	$C_6H_{12}O_6$
Crystal System	orthorhombic	trigonal	orthorhombic	orthorhombic	orthorhombic	orthorhombic
Space Group	$P2_12_12_1$ (#19)	$P3_2$ (#145)	$P2_12_12_1$ (#19)	$P2_12_12_1$ (#19)	$P2_12_12_1$ (#19)	$P2_12_12_1$ (#19)
a [Å]	4.918(1)	7.1749(13)	6.5949(11)	5.62999(16)	7.0800(3)	12.655(2)
b [Å]	11.925(2)	7.1749(13)	9.014(2)	7.5401(2)	9.8644(3)	7.771(1)
c [Å]	12.805(2)	12.7415(15)	12.720(2)	18.0919(5)	10.6156(4)	7.701(1)
α [°]	90	90	90	90	90	90
β [°]	90	90	90	90	90	90
γ [°]	90	120	90	90	90	90
Cell Volume [Å^3]	750.977	568.045	756.159	768.014	741.393	757.332
Z, Z'	Z=4, Z'=1	Z=3, Z'=1	Z=4, Z'=1	Z=4, Z'=1	Z=4, Z'=1	Z=4, Z'=1
Density [g/cm^3]	1.593	1.580	1.583	1.558	1.610	1.580
R-factor [%]	2.90	4.58	4.76	2.66	3.54	3.00

Table 2. Unit cell parameters of α-aldohexoses.

	α-D-glucose	α-D-talose	α-D-galactose
Formula	$C_6H_{12}O_6$	$C_6H_{12}O_6$	$C_6H_{12}O_6$
Crystal System	orthorhombic	orthorhombic	orthorhombic
Space Group	$P2_12_12_1$ (#19)	$P2_12_12_1$ (#19)	$P2_12_12_1$ (#19)
a [Å]	4.9379(4)	8.101(2)	5.8999(8)
b [Å]	10.3081(7)	12.126(2)	7.8433(12)
c [Å]	14.7882(11)	7.655(1)	15.685(4)
α [°]	90	90	90
β [°]	90	90	90
γ [°]	90	90	90
Cell Volume [Å^3]	752.725	751.972	725.818
Z, Z'	Z=4, Z'=1	Z=4, Z'=1	Z=4, Z'=1
Density [g/cm^3]	1.590	1.591	1.649
R-factor [%]	3.57	4.70	5.90

Table 3. Unit cell parameters of ketohexoses.

	β-D-fructose	β-D-psicose	α-L-sorbose	α-D-tagatose
Formula	$C_6H_{12}O_6$	$C_6H_{12}O_6$	$C_6H_{12}O_6$	$C_6H_{12}O_6$
Crystal System	orthorhombic	orthorhombic	orthorhombic	orthorhombic
Space Group	$P2_12_12_1$ (#19)	$P2_12_12_1$ (#19)	$P2_12_12_1$ (#19)	$P2_12_12_1$ (#19)
a [Å]	8.0818(4)	7.727(2)	6.545(2)	6.22010(10)
b [Å]	9.1394(4)	8.672(2)	18.062(7)	6.50220(10)
c [Å]	9.9546(5)	11.123(3)	6.310(2)	17.6629(4)
α [°]	90	90	90	90
β [°]	90	90	90	90
γ [°]	90	90	90	90
Cell Volume [$Å^3$]	735.275	745.336	745.942	714.364
Z, Z'	Z=4, Z'=1	Z=4, Z'=1	Z=4, Z'=1	Z=4, Z'=1
Density [g/cm^3]	1.627	1.605	1.604	1.675
R-factor [%]	2.03	3.95	3.70	2.47

From the Tables 1 to 3, it was found that, with the exception of β-D-altrose, all 12 remaining monosaccharides adopt an orthorhombic crystal system with the space group $P2_12_12_1$. In these 12 hexoses, the asymmetric unit contains four independent sugar molecules per unit cell. In contrast, β-D-altrose crystallizes in the trigonal system with the space group $P3_2$, and its unit cell contains three independent sugar molecules.

3.1. Crystal density

In this section, the crystal structures and crystal densities of six β-aldohexoses are discussed. Crystal density was chosen as a key parameter because it provides a quantitative measure of the degree of intermolecular packing. Among the examined β-aldohexoses, β-D-glucose exhibited the highest density at 1.610 g/cm³, followed by β-D-allose (1.593 g/cm³), β-D-gulose (1.583 g/cm³), β-D-altrose (1.580 g/cm³), β-D-galactose (1.580 g/cm³), and β-D-mannose (1.558 g/cm³). These variations in density are considered in relation to their respective packing arrangements. The packing structures of each monosaccharide are illustrated in the Figure 3, all projected along the *ac* plane. In these figures, yellow and green highlights denote axial OH groups, while pink highlights represent void spaces.

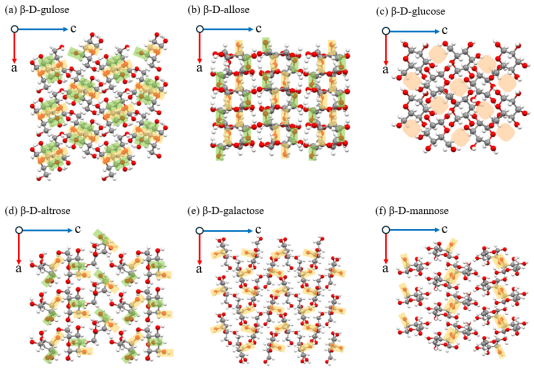


Figure 3. Packing diagrams of β-aldohexoses.
(a) β-D-gulose: OH group at C3 (yellow) and C4 (green).
(b) β-D-allose: OH group at C3 (yellow) and C6 (green).
(c) β-D-glucose: void space (pink).

(d) β-D-altrose: OH group at C2 (yellow) and C3 (green).
(e) β-D-galactose: OH group at C4 (yellow).
(f) β-D-mannose: OH group at C4 (yellow).

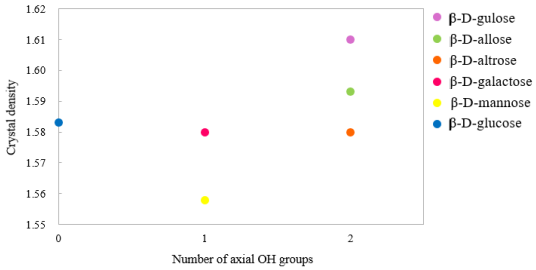


Figure 4. Relationship between crystal density and the number of axial OH groups.

In discussing packing arrangements, particular attention was given to OH groups occupying axial positions in each β-aldohexose. The counts are: β-D-gulose: 2; β-D-allose: 1 (2); β-D-glucose: 0; β-D-altrose: 2; β-D-galactose: 1; β-D-mannose: 1. In β-D-allose, only the OH group at C2 is axial; however, the C6 OH—though part of an equatorially oriented CH_2OH moiety—projects perpendicularly to the ring and was treated as functionally axial.

As shown in Figure 3, β-D-gulose possesses two axial OH groups, enabling an interlocking arrangement with adjacent sugar molecules reminiscent of a "tenon-and-mortise" joint, resulting in a tightly packed structure. This packing motif is considered to contribute to its high crystal density. β-D-allose, which effectively contains two axial OH groups, adopts a similar configuration; however, because the OH group at C6 is part of a CH_2OH moiety, its greater steric bulk likely results in a slightly lower density than that of gulose. In β-D-glucose, all OH groups adopt equatorial orientations, which minimizes steric hindrance, however, repulsive interactions between hydrogen atoms of neighboring molecules appear to reduce the density further. β-D-altrose also contains two axial OH groups, but its trigonal ($P3_2$) crystal system features an extended repeat along the c-axis, which hinders the formation of the tenon-and-mortise arrangement and prevents densification. In contrast, β-D-galactose and β-D-mannose each possess only one axial OH group, limiting efficient intermolecular complementarity and leading to the presence of voids, thereby yielding the lowest crystal densities among the six β-aldohexoses examined. To strengthen the connection between the structural models and quantitative results, Figure 4 illustrates the relationship between crystal density and the number of axial OH groups. While this plot captures the overall trend, β-D-altrose deviates from the expected increase in density with two axial OH groups. This anomaly is consistent with its packing diagram (Figure 3), where the $P3_2$ symmetry elongates the c-axis repeat and inhibits efficient interlocking, visually confirming the structural origin of its lower density.

Based on these results, in β-aldohexoses, crystal density is strongly influenced by the number of axial OH groups. When two are present, optimal steric "interlocking" between neighboring molecules minimizes void space, yielding dense packing through geometric optimization of molecular orientation. Conversely, deviations from two reduce contact area and orientational matching, thereby increasing lattice voids and lowering density.

3.2. Molecular orbital calculations

In this section, molecular orbital (MO) calculations were conducted for 13 hexoses to evaluate the strength of hydrogen bonds formed between a central molecule and its surrounding neighbors, expressed as BOP values. The results are presented in Tables 4, 6 and 7. Although both donor- and acceptor-type hydrogen bonds exist, they are crystallographically equivalent; therefore, only the donor-type hydrogen bond data are shown here as representative. In the tables, the oxygen atom index indicates the donor

atom from which the hydrogen bond originates—for example, a hydrogen bond from O1 to O4 is abbreviated simply as "O1." In addition, the value shown to the right of each BOP represents the percentage deviation from the average BOP for that sugar, with units given in %. For instance, in Table 4, the BOP from O1 in β-D-allose is 0.0638 electrons, which is 80.9 % higher than the molecular average of 0.0353 electrons, and is therefore denoted as "+80.9." To facilitate visual interpretation, the highest BOP value in each table is highlighted in orange, the lowest in light blue, and the second to fourth highest values are shaded in varying tones of gray. As shown in Tables 4–6, more than half of the BOP values fall within the 10^{-2} order of magnitude, validating them as reasonable indicators of hydrogen bond strength. The 13 hexoses are here grouped into β-aldohexoses, α-aldohexoses, and ketohexoses to facilitate systematic discussion.

(I) β-aldohexose

Table 4. The BOP values for β-aldohexoses, along with their total and average values.

O number	BOP (H-Donor)											
	β-D-allose		β-D-altrose		β-D-glucose		β-D-mannose		β-D-gulose		β-D-galactose	
O1	0.0638	**+80.9**	0.0237	**-16.4**	0.0432	**+92.2**	0.0336	**+17.7**	0.0353	**+63.7**	0.0811	**+67.6**
O2	0.0288	**-18.3**	0.0265	**-6.5**	0.0135	**-39.9**	0.0233	**-18.4**	0.0126	**-41.6**	0.0381	**-21.3**
O3	0.0327	**-7.3**	0.0330	**+16.4**	0.0097	**-56.8**	0.0145	**-49.2**	0.0354	**+64.2**	0.0302	**-37.6**
O4	0.0352	**-0.2**	0.0276	**-2.6**			0.0399	**+39.8**	0.0245	**+13.6**	0.0416	**-14.0**
O6	0.0158	**-55.2**	0.0309	**+9.0**	0.0235	**+4.6**	0.0314	**+10.0**	0.0277	**+28.5**	0.0510	**+5.4**
SUM	0.1763		0.1417		0.0899		0.1427		0.1078		0.2420	
AVG	0.0353		0.0283		0.0225		0.0285		0.0216		0.0484	

Table 5. The hydrogen bond distances at O1 and their difference from the molecular average in β-aldohexoses. Distances are given in Å.
Δ = H-bond distance (O1) − Molecular average H-bond distance.

	β-D-allose	β-D-altrose	β-D-glucose	β-D-mannose	β-D-gulose	β-D-galactose
H-bond distance (O1)	1.6786	1.9730	1.7878	1.9223	1.9282	1.6493
Molecular average H-bond distance	1.9425	1.9430	2.0143	1.9750	2.0074	1.8607
Difference from average Δ	-0.2639	0.0300	-0.2265	-0.0527	-0.0792	-0.2114

As shown in Table 4, a comparison of the overall BOP values for β-aldohexoses reveals that O1 consistently exhibits the highest values. This trend is likely attributable to the molecular architecture of hexoses. The anomeric oxygen (O1), located adjacent to the bridging oxygen (O5) and positioned at the terminus of the pyranose ring, experiences less steric hindrance from neighboring substituents than other hydroxyl groups (O2 to O4). Consequently, hydrogen bond formation with adjacent molecules is spatially more favorable, leading to elevated BOP values. This interpretation is further supported by Table 5, in which O1 consistently shows shorter hydrogen bond distances than the molecular average. A representative example is β-D-allose. As shown in Figure 3, β-D-allose forms its principal hydrogen-bond network along the a-axis, bringing neighboring molecules into closer proximity. This structural feature shortens the O1–H···O distance (Table 5), and the corresponding BOP value for O1 becomes the largest among all donor sites. This case clearly illustrates how the dominant packing direction visible in the molecular arrangement is directly reflected in the quantitative BOP results.

In contrast, β-D-altrose represents a notable exception to this trend. Its trigonal ($P3_2$) crystal symmetry imposes an extended repeat along the c axis, altering the orientation and geometric

accessibility of the O1 hydroxyl group. As a result, the O1–H· · · O distance is longer than in the other β-aldohexoses (Table 5), yielding a lower BOP value.

(II) α-aldohexose

Table 6. The BOP values for α-aldohexoses, along with their total and average values.

O number	BOP (H-Donor)					
	α-D-glucose		α-D-talose		α-D-galactose	
O1	0.0291	-17.19	0.0150	-22.20	0.0819	103.23
O2	0.0412	17.25	0.0209	8.40	0.0246	-38.96
O3	0.0372	5.86	0.0206	6.85	0.0303	-24.81
O4	0.0302	-14.06	0.0270	40.04	0.0313	-22.33
O6	0.0380	8.14	0.0129	-33.09	0.0334	-17.12
SUM	0.1757		0.0964		0.2015	
AVG	0.0351		0.0193		0.0403	

As shown in Table 5, α-aldohexoses did not display the distinct trend in BOP values observed for β-aldohexoses. This outcome can be attributed to differences in the stereochemical orientation of the anomeric OH group. In α-anomers, the anomeric OH adopts an axial orientation, in contrast to the equatorial orientation in β-anomers, which extends parallel to the six-membered ring. This axial arrangement imposes geometric constraints on both the distance and relative orientation to neighboring molecules, resulting in greater variability in the directionality and strength of hydrogen bonding. Consequently, no single oxygen atom exhibited a consistently dominant BOP value in α-aldohexoses. Collectively, these findings underscore that the structural differences between β- and α-aldohexoses highlight the critical role of the OH group orientation in governing hydrogen bond formation.

(III) ketohexose

Table 7. The BOP values for ketohexoses, along with their total and average values.

O number	BOP (H-Donor)							
	β-D-fructose		β-D-psicose		α-L-sorbose		α-D-tagatose	
O1	0.0220	-17.10	0.0222	4.52	0.0363	-16.40	0.0191	-28.83
O2	0.0469	76.71	0.0273	28.53	0.0427	-1.66	0.0205	-23.62
O3	0.0223	-15.98	0.0154	-27.50	0.0605	39.34	0.0358	33.38
O4	0.0153	-42.35	0.0179	-15.73	0.0409	-5.80	0.0328	22.21
O5	0.0262	-1.28	0.0234	10.17	0.0367	-15.48	0.0260	-3.13
SUM	0.1327		0.1062		0.2171		0.1342	
AVG	0.0265		0.0212		0.0434		0.0268	

As shown in Table 6, ketohexoses exhibited a consistent trend in which the BOP value for the O1 atom, bound to the C1 position, was the lowest among all hydroxyl groups. This feature is attributable to the unique structural arrangement in which both an OH group and a CH_2OH group are positioned adjacent to the anomeric center. The close proximity of these two bulky functional groups induces significant steric interactions, which in turn spatially restrict the formation of hydrogen bonds, ultimately leading to the observed reduction in BOP values.

Overall, these results show that BOP values are strongly influenced by the orientation of the OH groups and nearby substituents. In β-aldohexoses, the equatorial and sterically open anomeric OH promotes strong hydrogen bonding, elevating O1 values. In α-aldohexoses, the axial orientation imposes spatial constraints, preventing a consistent dominance for any oxygen atom. In ketohexoses, steric interference from two adjacent functional groups at the anomeric center weakens hydrogen bonds. Thus, the OH group orientation and local structural features are key determinants of hydrogen bond network strength in the crystal lattice.

4. Conclusion

This study combined crystal structure analysis with DV-Xα method to quantify how the OH group stereochemistry affects crystal density and hydrogen bond strength in hexoses. In β-aldohexoses, the highest crystal densities were observed when two axial OH groups were present, as this arrangement promotes efficient molecular interlocking and minimizes void space. Deviations from this count reduce packing efficiency and consequently lower density.

BOP analysis revealed that in β-aldohexoses, the equatorial orientation of the anomeric OH favored strong hydrogen bonding at O1, whereas in α-aldohexoses, the axial orientation imposed spatial constraints, eliminating a consistent site preference. In ketohexoses, O1 showed the lowest BOP values due to steric interference between the anomeric OH and CH_2OH groups.

These results highlight the pivotal role of OH group orientation and local structural features in dictating crystal packing efficiency and hydrogen bond network strength. These findings provide a structural basis that may be useful in considering future development of sugar based functional materials. As a next step, we aim to explore the single-crystal growth of candidate sugars that show potential for such applications, in order to further examine how their intermolecular interactions can be utilized.

Acknowledgements

I would like to express my sincere gratitude to M. Matsumoto and T. Nishimura for their valuable discussions and insightful comments, which greatly helped me refine the ideas and analyses presented in this study. Their guidance and encouragement were instrumental throughout the research process.

References

[1] International Society of Rare Sugars: https://www.isrs.kagawa-u.ac.jp
[2] Matsuo T, Baba Y, Hashiguchi M, Takeshita K, Izumori K, Suzuki H. Dietary D -psicose, a C-3 epimer of D -fructose, suppresses the activity of hepatic lipogenic enzymes in rats. *Asia Pac J Clin Nutr* 2001;10:233–7. https://doi.org/10.1046/j.1440-6047.2001.00246.x.
[3] Matsuo T, Tanaka T, Hashiguchi M, Izumori K, Suzuki H. Metabolic effects of D-psicose in rats: studies on faecal and urinary excretion and caecal fermentation. *Asia Pac J Clin Nutr* 2003;12:225–31.
[4] Livesey G, Brown JC. D-Tagatose Is a Bulk Sweetener with Zero Energy Determined in Rats. *J Nutr* 1996;126:1601–9. https://doi.org/10.1093/jn/126.6.1601.
[5] Lu Y, Levin GV, Donner TW. Tagatose, a new antidiabetic and obesity control drug. *Diabetes Obes Metab* 2008;10:109–34. https://doi.org/10.1111/j.1463-1326.2007.00799.x.
[6] Nurhasanah S, Muhaimin, Pyopyash SA, Zaida, Pangawikan ADP. Enhancing Functional Foods with Plant Extracts: A Study on Gummy Candies Containing Sungkai Leaf Extract. *Adv Sustain Sci Eng Technol* 2025;7:02502024. https://doi.org/10.26877/tjdgyw23.
[7] Matsuo T, Suzuki H, Hashiguchi M, Izumori K. D-Psicose Is a Rare Sugar That Provides No Energy to Growing Rats. *J Nutr Sci Vitaminol* (Tokyo) 2002;48:77–80. https://doi.org/10.3177/jnsv.48.77.
[8] Tohi Y, Taoka R, Zhang X, Matsuoka Y, Yoshihara A, Ibuki E, et al. Antitumor Effects of Orally Administered Rare Sugar D-Allose in Bladder Cancer. *Int J Mol Sci* 2022;23:6771.

Kode Bidang Diubah

https://doi.org/10.3390/ijms23126771.
[9] Hoshikawa H, Indo K, Mori T, Mori N. Enhancement of the radiation effects by d-allose in head and neck cancer cells. *Cancer Lett* 2011;306:60–6. https://doi.org/10.1016/j.canlet.2011.02.032.
[10] Yamaguchi F, Takata M, Kamitori K, Nonaka M, Dong Y, Sui L, et al. Rare sugar D-allose induces specific up-regulation of TXNIP and subsequent G1 cell cycle arrest in hepatocellular carcinoma cells by stabilization of p27kip1. *Int J Oncol* 2008;32:377–85.
[11] Mochizuki S, Fukumoto T, Ohara T, Ohtani K, Yoshihara A, Shigematsu Y, et al. The rare sugar d-tagatose protects plants from downy mildews and is a safe fungicidal agrochemical. *Commun Biol* 2020;3:423. https://doi.org/10.1038/s42003-020-01133-7.
[12] Pal KB, Sarkar V, Mukhopadhyay B. Hydrogen bonding-induced conformational change in a crystalline sugar derivative. *CrystEngComm* 2016;18:1156–63. https://doi.org/10.1039/C5CE01893E.
[13] Pindelska E, Mogilnicki MA, Jaśkowska J, Madura ID. Multimethod Approach to Understanding the Different Affinity for the 5-HT_{1A} Receptor of Three Regioisomers of Novel Arylpiperazine Salicylamide Ligand. *Cryst Growth Des* 2023;23:5827–38. https://doi.org/10.1021/acs.cgd.3c00438.
[14] Kroon-Batenburg LMJ, Van Der Sluis P, Kanters JA. Structure of β-D-allose, C6H12O6. *Acta Crystallogr C* 1984;40:1863–5. https://doi.org/10.1107/S0108270184009859.
[15] Watanabe Y, Yoshida H, Takeda K, Ishi T, Kamitori S. β- D -Altrose. *Acta Crystallogr Sect E Struct Rep Online* 2009;65:o280–o280. https://doi.org/10.1107/S1600536809000397.
[16] Kouwijzer MLCE, Van Eijck BP, Kooijman H, Kroon J. An extension of the *GROMOS* force field for carbohydrates, resulting in improvement of the crystal structure determination of α- D -galactose. *Acta Crystallogr B* 1995;51:209–20. https://doi.org/10.1107/S0108768194011262.
[17] Patyk E, Jenczak A, Katrusiak A. CCDC 1450809: Experimental Crystal Structure Determination 2016. https://doi.org/10.5517/CCDC.CSD.CC1KPP97.
[18] Ishii T, Ohga S, Fukada K, Morimoto K, Sakane G. β- D -Gulose. *Acta Crystallogr Sect E Struct Rep Online* 2014;70:o569–o569. https://doi.org/10.1107/S1600536814008046.
[19] Longchambon F, Ohannessian J, Avenel D, Neuman A. Structure cristalline du β- D -galactose et de l'α- L -fucose. *Acta Crystallogr B* 1975;31:2623–7. https://doi.org/10.1107/S0567740875008333.
[20] Fronczek FR. CCDC 1500503: Experimental Crystal Structure Determination 2016. https://doi.org/10.5517/CCDC.CSD.CC1MCDBQ.
[21] Hansen LK, Hordvik A, Näsäkkälä E, Kjekshus A, Rakke T, Andresen AF. The Molecular Structure of alpha-D-Talose. *Acta Chem Scand* 1977;31a:187–91. https://doi.org/10.3891/acta.chem.scand.31a-0187.
[22] Fronczek FR. CCDC 1902789: Experimental Crystal Structure Determination 2019. https://doi.org/10.5517/CCDC.CSD.CC21W098.
[23] Fukada K, Ishii T, Tanaka K, Yamaji M, Yamaoka Y, Kobashi K, et al. Crystal Structure, Solubility, and Mutarotation of the Rare Monosaccharide D -Psicose. *Bull Chem Soc Jpn* 2010;83:1193–7. https://doi.org/10.1246/bcsj.20100148.
[24] Nordenson S, Takagi S, Jeffrey GA. α-L-Sorbopyranose: a neutron diffraction refinement. *Acta Crystallogr B* 1979;35:1005–7. https://doi.org/10.1107/S0567740879005422.
[25] Punzo F, Watkin DJ, Fleet GWJ. CCDC 738284: Experimental Crystal Structure Determination 2009. https://doi.org/10.5517/CCSS7MD.
[26] Ishii T. *Crystal structure of rare sugars* 2024. https://doi.org/10.32285/glycoforum.27A23.
[27] Ishii T, Ogasawara K, Sakane G. Exploring spin states and ligand field splitting in metal complexes: a theoretical analysis of spin–orbital interactions and magnetic properties. *Dalton Trans* 2024;53:7175–89. https://doi.org/10.1039/D4DT00329B.
[28] Nishimura T, Toba T, Sakane G, Ishii T. Periodicity of Superatomic Hybrid Orbitals in Substituted Superatoms and Superatomic-like X@Ga12 (X = Li~Kr) Clusters. *Crystals* 2022;12:543. https://doi.org/10.3390/cryst12040543.

[29] Nishimura T, Kodama T, Genta S, Ishii T. Transition metals doped effects for the crystal stabilization of the cerium oxides with the first principle calculation. *Sci Rep* 2022;12:10103. https://doi.org/10.1038/s41598-022-14180-3.